*Mon. Not. R. astr. Soc.* (1989) **238**, 97–113

# Analysis of the photometric variability of WR40★

E. Gosset,[1,2] J.-M. Vreux,[2] J. Manfroid,[2]† C. Sterken,[3]† E. N. Walker[4] and R. Haefner[5]

[1] *European Southern Observatory, Karl-Schwarzschild-Str., 2, D-8046 Garching bei München, FRG*

[2] *Institut d'Astrophysique, Université de Liège, B-4200 Cointe Ougrée, Belgium*

[3] *Astrophysical Institute, Vrije Universiteit Brussel, Pleinlaan, 2, B-1050 Brussels, Belgium*

[4] *Teutneys Cottage, Old Road, Herstmonceux, East Sussex BN27 1RP*

[5] *Universitäts-Sternwarte, Scheinerstr., 1, D-8000 München 80, FRG*

Accepted 1988 October 14. Received 1988 October 7; in original form 1988 June 9

**Summary.** New photometric data on the Wolf–Rayet star WR40 are presented and, together with data already published, are analysed in a detailed and homogeneous manner in order to investigate the variability of the star. Good evidence is presented for the existence of a periodicity $P = 6.250 \pm 0.078 (1\sigma)$ day ($\nu = 0.160 \pm 0.002$ day$^{-1}$) with a semi-amplitude of 0.010 mag in the Strömgren *b* filter. Only part of the 0.1 mag peak-to-peak variation of the star can be explained in this way and other interesting features of the variability are outlined. The physical origin of the periodicity is discussed.

## 1 Introduction

The WN8 star WR40 (HD 96548, $V \sim 7.8$) is intriguing in many aspects. Among the galactic Wolf–Rayets, 15 are surrounded by arcs of nebulosity. The latter, usually called 'ring nebulae', are centred on, and ionized by, the WR star. These remarkable signatures of the interaction between WR stars and the interstellar medium have been extensively studied by Chu, Treffers & Kwitter (1983, and papers quoted therein) who introduce a classification in three categories based on the formation mechanism. These are E (stellar ejecta), W (wind-blown interstellar bubbles) and R (radiatively excited H II regions). In their survey, they identify only two nebulae of class E, RCW58 and M1-67, linked respectively to WR40 (=HD 96548) and WR124 (=209 BAC). As it has been argued recently that the latter is a planetary nebula and not a genuine Population I Wolf–Rayet (van der Hucht *et al.* 1985), WR40 remains a unique example of an undisputed galactic WR star surrounded by stellar ejecta. Two other facts have

★ Partly based on observations collected at ESO, Chile.

† Senior Research Associate, Belgian FNRS/NFWO.

also drawn the attention on WR40: its relatively large distance from the galactic plane ($Z = -339$ pc; van der Hucht *et al.* 1988) and its variability. These three characteristics point to the fact that WR40 could be an object in the WR+compact class, the existence of which had been suggested by theoreticians such as van den Heuvel & Heise (1972), Tutukov & Yungelson (1973) and de Loore & de Grève (1975). WR40 was indeed claimed to be such a system by Moffat & Isserstedt (1980, to be referred to as MI), who, on the basis of extensive photometry and spectroscopy, find a possible period of 4.762 day (frequency $\nu = 0.210$ day$^{-1}$) with a full amplitude of 0.04 mag superimposed on random noise ( ~ 0.02 mag rms). The coudé spectra show radial velocity variations with a semi-amplitude of 8–10 km s$^{-1}$. Later on, Moffat (1983) revised the period from 4.762 day down to 4.158 day ($\nu = 0.241$ day$^{-1}$) on the basis of new radial velocity data. Two years later, WR40 was reinvestigated by Smith, Lloyd & Walker (1985): using their own data, as well as the published data of MI, they find little evidence for the period mentioned above. Instead, they find evidence for a period of 5.879 day ($\nu = 0.170$ day$^{-1}$) or its 1-day aliases at 1.204 day ($\nu = 0.831$ day$^{-1}$) or 0.855 day ($\nu = 1.170$ day$^{-1}$). The latter is preferred when they analyse the only set of data which regularly contains multiple observations per night, i.e. when they analyse the only set of data enabling the search for such a high frequency. Nevertheless, the data do not allow a definitive choice. In 1986, van Genderen, van der Hucht & Steemers (1987) observed WR40 in the *VLBUW* photometric system of Walraven. Due to the insufficient number of observations, they do not try any independent period search from their data: they simply plot them in a phase diagram using the suggested periods, and conclude that they cannot support any of the proposed periods, probably due to a large intrinsic scatter. We have more data covering roughly the same epoch (the first months of 1986). They will be analysed in Section 3. Quite recently, Lamontagne & Moffat (1987, to be referred to as LM) rediscussed the variability of WR40 on the basis of new photometric observations (the polarimetric observations of Drissen *et al.* (1987) leading to a null result: no periodicity is found as in any of the WNL investigated with that technique). They claim that their new photometric data yield a best period of 4.7 day ($\nu = 0.21$ day$^{-1}$) 'in support of the best period found previously by MI'. The problem is that they also write that a 'light curve based on this period in fig. 3(d) shows a single wave of amplitude ~ 0.04 mag' while the original paper of MI claimed a double wave per cycle for that period. In fact, the reason for this double wave is that 'the best consistent period longer than two days' derived from the photometric data sets analysed in the MI paper 'is $P = 2.4$ day' ($\nu = 0.42$ day$^{-1}$). They finally choose twice that period for consistency with their radial velocity data which are 'suggestive of a typical time-scale of 4–5 day'. As a consequence, instead of supporting the best period previously found, these new data could as well be considered as an example of a change in the periodicity. One of us (Vreux 1987) has recently drawn the attention to different peculiarities exhibited by the variability of many of the so-called WR+c, a change of the apparent period with the epoch of observation being one of them. If confirmed, such peculiarities will have to be evaluated in the frame of the controversy he has raised about the interpretation of the

**Table 1.** Journal of the observations relevant to the new photometric data.

| # | Run | JD(2440000+) | Telescope | Observer | N | Group | Data set |
|---|---|---|---|---|---|---|---|
| 1 | January 85 | 6067-6098 | ESO 50cm | H. Duerbeck* | 23 | 1 | II |
| 2 | February 85 | 6099-6113 | Danish 50cm | C. Sterken | 15 | 2 | |
| 3 | March 85 | 6135-6154 | ESO 50cm | O. Stahl* | 30 | 1 | II |
| 4 | December 85 | 6424-6443 | Danish 50cm | F.-J. Zickgraf* | 18 | 2 | III |
| 5 | February 86 | 6475-6496 | Danish 50cm | M. Burger* | 23 | 2 | III |
| 6 | March 86 | 6498-6519 | Danish 50cm | A. Jorissen* | 25 | 2 | III |
| 7 | June 86 | 6582-6609 | Danish 50cm | D. Steenman* | 13 | 2 | III |
| 8 | April 87 | 6884-6895 | ESO 50cm | J. Manfroid | 489 | 3 | I |
| 9 | May 87 | 6939-6942 | ESO 50cm | R. Haefner | 48 | 3 | I |

Remarks to table 1

* Observer for the "Long Term Photometry of Variables" project

variability itself: binarity or intrinsic variability of a single object? This question ultimately addresses the number ratio of single to binary WR stars and thus the relative importance of the evolutionary channels leading to WR stars. Due to the fundamental interest of that question, and the evident confusion among the previous analyses, we have decided to collect new data on WR40 and to re-analyse all the previously available data in a systematic and self-consistent way. Indeed some previous analyses were performed with only one technique, and it is not excluded that this simple fact could induce a spurious apparent variation of the period. This is also why we will try to quantify as much as possible the different results.

## 2 Observations and reduction

The observations were carried out at ESO during several runs at the ESO 50-cm and the Danish 50-cm telescopes. The ESO telescope was equipped with a one-channel photometer, the Danish telescope with a four-channel one especially designed for the Strömgren photometry.

Most of the observing runs were made in the framework of the 'Long-term Photometry of Variables' project (Sterken 1983). In 1987 April, a run was especially dedicated to WR40 and a few other objects (see, for example, Manfroid, Gosset & Vreux 1987).

Table 1 presents a journal of the new observations concerned by our analysis. The different columns give

A sequence number of the run.
The approximate epoch.
The relevant Julian date.
The telescope used.
The observer.
The number of measurements.
A group identifier (see below).
A dataset identifier (see below and Section 3).

The reduction procedure is based on the method outlined by Manfroid (1985). Because of (i) the strong dependence of the data on the filter pass-band and (ii) the peculiar colour indices of Wolf–Rayet stars, we did not consider colour transformations. This explains systematic effects between different telescopes. The data from runs No. 1 to No. 7 were kept in two groups (1, 2) according to the characteristics of the natural system.

One observation of group 1 and/or 2 consists of a short sequence $C_1VC_2$ where $C_1$ and $C_2$ are the comparison stars (HD 96287 and HD 96568) and V is the Wolf–Rayet star (WR40).

The last runs (No. 8 and No. 9) were considered separately (group 3) because many more data were secured. Moreover, the adopted sequence was $C_1C_2VC_1C_2VC_1C_2VC_1C_2V$ usually repeated four times. Only the Strömgren *b* filter was utilized. Each individual measurement consisted of short integrations totalling 80–120 s and an entire sequence lasted between 20 and 30 min. Typically, three such quartets of sequences were performed every night so that eventual light variations on a time-scale of a few hours would be detected.

The data issued from the different runs have been collected in three datasets in order to preserve the homogeneity indispensable for the subsequent analysis. Dataset I is formed by the *b* filter data from runs No. 8 and No. 9. The quartets of sequences have been averaged in such a way that we obtain 35 measurements. They are given in Table 2 in the form of differential magnitudes between WR40 and the mean of the comparison stars. Dataset II gathers the *b* and *y* filter data from runs No. 1 and No. 3; the relevant differential magnitudes are given in Table 3. Finally, *b* and *y* filter data from runs Nos 4–7 constitute dataset III which is to be found in

**Table 2.** Observations contained in dataset I.

| JD 2440000+ | $b$ |
|---|---|
| 6884.6152 | 0.6516 |
| 6884.6972 | 0.6626 |
| 6884.8052 | 0.6835 |
| 6885.6241 | 0.6870 |
| 6885.6971 | 0.6971 |
| 6885.7862 | 0.6904 |
| 6886.5452 | 0.6370 |
| 6886.6502 | 0.6334 |
| 6886.7675 | 0.6356 |
| 6887.5521 | 0.6737 |
| 6887.6590 | 0.6804 |
| 6887.8004 | 0.6840 |
| 6888.5463 | 0.6766 |
| 6888.7087 | 0.6659 |
| 6889.5564 | 0.6363 |
| 6889.6789 | 0.6254 |
| 6889.8088 | 0.6282 |
| 6890.6101 | 0.6690 |
| 6891.5485 | 0.6570 |
| 6891.6705 | 0.6487 |
| 6891.8001 | 0.6542 |
| 6892.5514 | 0.6769 |
| 6892.6507 | 0.6786 |
| 6892.7983 | 0.6815 |
| 6893.5246 | 0.6667 |
| 6893.6341 | 0.6717 |
| 6894.5537 | 0.6483 |
| 6894.6603 | 0.6532 |
| 6894.7925 | 0.6635 |
| 6895.5472 | 0.6661 |
| 6895.6873 | 0.6580 |
| 6895.7738 | 0.6560 |
| 6939.6606 | 0.6712 |
| 6941.6439 | 0.7007 |
| 6942.6216 | 0.6609 |

**Table 3.** Observations contained in dataset II.

| JD 2440000+ | $b-y$ | $y$ | JD 2440000+ | $b-y$ | $y$ |
|---|---|---|---|---|---|
| 6067.7985 | −0.1237 | 0.8706 | 6139.6687 | −0.1447 | 0.9271 |
| 6068.7894 | −0.1150 | 0.8352 | 6140.5982 | −0.1447 | 0.9067 |
| 6069.7803 | −0.1224 | 0.8498 | 6140.7766 | −0.1430 | 0.9051 |
| 6070.8348 | −0.1250 | 0.9034 | 6141.5613 | −0.1291 | 0.8682 |
| 6071.7736 | −0.1293 | 0.9041 | 6141.7051 | −0.1414 | 0.8942 |
| 6072.8019 | −0.1389 | 0.9419 | 6141.7843 | −0.1500 | 0.9231 |
| 6077.7929 | −0.1266 | 0.8737 | 6142.5685 | −0.1345 | 0.9033 |
| 6078.8330 | −0.1608 | 0.9344 | 6142.6875 | −0.1399 | 0.9077 |
| 6079.7979 | −0.1214 | 0.8923 | 6142.7990 | −0.1465 | 0.9181 |
| 6080.8648 | −0.1328 | 0.9126 | 6143.6280 | −0.1330 | 0.8863 |
| 6081.7938 | −0.1150 | 0.8643 | 6144.6132 | −0.1285 | 0.9049 |
| 6082.8179 | −0.1190 | 0.8813 | 6144.7864 | −0.1257 | 0.8932 |
| 6087.8571 | −0.1152 | 0.8618 | 6145.5852 | −0.1309 | 0.8666 |
| 6088.7936 | −0.1207 | 0.8514 | 6145.8027 | −0.1380 | 0.8724 |
| 6089.7567 | −0.1403 | 0.9373 | 6146.5449 | −0.1353 | 0.8778 |
| 6091.7378 | −0.1176 | 0.8962 | 6146.7787 | −0.1486 | 0.8928 |
| 6092.7714 | −0.1155 | 0.8650 | 6148.6816 | −0.1474 | 0.8974 |
| 6093.8310 | −0.1312 | 0.9034 | 6149.6004 | −0.1361 | 0.8893 |
| 6094.7658 | −0.1082 | 0.8462 | 6149.7743 | −0.1466 | 0.8919 |
| 6095.7514 | −0.1237 | 0.8693 | 6150.5898 | −0.1490 | 0.8994 |
| 6096.7694 | −0.1437 | 0.9223 | 6151.7141 | −0.1186 | 0.8711 |
| 6097.7514 | −0.1228 | 0.8884 | 6152.5344 | −0.1484 | 0.9081 |
| 6098.7705 | −0.1167 | 0.8658 | 6152.7362 | −0.1399 | 0.8843 |
| 6135.7771 | −0.1378 | 0.9267 | 6153.6022 | −0.1482 | 0.9030 |
| 6136.7123 | −0.1326 | 0.9021 | 6154.5705 | −0.1682 | 0.9406 |
| 6137.7412 | −0.1364 | 0.9012 | 6154.7177 | −0.1368 | 0.9074 |
| 6138.6687 | −0.1422 | 0.8951 | | | |

Table 4. Table 5 shows the $b$ and $y$ filter data from run No. 2. They are too isolated relative to the observations of dataset III and not numerous enough to permit a secure transformation and an inclusion in dataset II. Consequently, they were considered separately (see Section 3.3).

**Table 4.** Observations contained in dataset III.

| JD 2440000+ | $b-y$ | $y$ | JD 2440000+ | $b-y$ | $y$ |
|---|---|---|---|---|---|
| 6424.7890 | −0.1803 | 0.9091 | 6496.7682 | −0.1821 | 0.8586 |
| 6425.7924 | −0.1803 | 0.9169 | 6498.7996 | −0.1756 | 0.8721 |
| 6427.8456 | −0.1715 | 0.9026 | 6499.8736 | −0.1644 | 0.8452 |
| 6428.8139 | −0.1992 | 0.9371 | 6500.7523 | −0.1628 | 0.8398 |
| 6429.7876 | −0.1720 | 0.8756 | 6501.7546 | −0.1656 | 0.8372 |
| 6430.7884 | −0.1927 | 0.9510 | 6502.7658 | −0.1804 | 0.8576 |
| 6431.7792 | −0.1892 | 0.9436 | 6503.7088 | −0.1896 | 0.9021 |
| 6432.7916 | −0.1684 | 0.8852 | 6503.7951 | −0.2000 | 0.9122 |
| 6433.7787 | −0.1888 | 0.9310 | 6504.7925 | −0.1887 | 0.9435 |
| 6434.7643 | −0.1947 | 0.9556 | 6505.7311 | −0.1691 | 0.8976 |
| 6435.7621 | −0.1750 | 0.9225 | 6505.8297 | −0.1700 | 0.8927 |
| 6436.7685 | −0.1647 | 0.8860 | 6506.6255 | −0.1634 | 0.8506 |
| 6437.7579 | −0.1716 | 0.8795 | 6506.7935 | −0.1698 | 0.8666 |
| 6439.7737 | −0.1958 | 0.9292 | 6507.6491 | −0.1971 | 0.9154 |
| 6440.7793 | −0.1953 | 0.9390 | 6507.8153 | −0.1944 | 0.9167 |
| 6441.7742 | −0.1645 | 0.8733 | 6508.7689 | −0.1947 | 0.9532 |
| 6442.7946 | −0.1716 | 0.8910 | 6509.7559 | −0.1911 | 0.9520 |
| 6443.7567 | −0.1825 | 0.8923 | 6510.7677 | −0.1782 | 0.8973 |
| 6475.7673 | −0.1812 | 0.8851 | 6511.7389 | −0.1809 | 0.8786 |
| 6476.8102 | −0.1847 | 0.9576 | 6512.7481 | −0.1911 | 0.8990 |
| 6477.7420 | −0.1864 | 0.9348 | 6513.7305 | −0.1980 | 0.9516 |
| 6478.7906 | −0.1871 | 0.9220 | 6516.7727 | −0.1802 | 0.8728 |
| 6480.7223 | −0.1711 | 0.8703 | 6517.7510 | −0.1808 | 0.9240 |
| 6480.8257 | −0.1803 | 0.8770 | 6518.7083 | −0.1524 | 0.8182 |
| 6481.6790 | −0.1863 | 0.8825 | 6518.8129 | −0.1607 | 0.8237 |
| 6481.8103 | −0.1858 | 0.8875 | 6519.6685 | −0.1620 | 0.8592 |
| 6482.7233 | −0.1623 | 0.8432 | 6582.5653 | −0.1925 | 0.9116 |
| 6483.7489 | −0.1818 | 0.8979 | 6583.6513 | −0.1950 | 0.9340 |
| 6484.7929 | −0.1644 | 0.8713 | 6584.5547 | −0.1718 | 0.8534 |
| 6485.8341 | −0.1802 | 0.8717 | 6585.5553 | −0.1896 | 0.9225 |
| 6486.7428 | −0.1592 | 0.8330 | 6587.5875 | −0.1688 | 0.8983 |
| 6487.7513 | −0.1758 | 0.8456 | 6588.5479 | −0.1825 | 0.8874 |
| 6488.7693 | −0.1792 | 0.8752 | 6589.5757 | −0.1725 | 0.8994 |
| 6489.7436 | −0.1747 | 0.8708 | 6604.5560 | −0.1608 | 0.8727 |
| 6490.7767 | −0.1632 | 0.8876 | 6605.5713 | −0.1682 | 0.8557 |
| 6491.7436 | −0.1703 | 0.8404 | 6606.5601 | −0.1921 | 0.9085 |
| 6492.7406 | −0.1851 | 0.8938 | 6607.4929 | −0.1727 | 0.8867 |
| 6493.7527 | −0.1923 | 0.9381 | 6608.5562 | −0.1798 | 0.9154 |
| 6494.7304 | −0.1626 | 0.8784 | 6609.5023 | −0.1858 | 0.9265 |
| 6495.7347 | −0.1787 | 0.8958 | | | |

## 3 The photometric variability of WR40

### 3.1 ANALYSIS OF THE NEW DATA

#### *3.1.1 Dataset I*

Dataset I consists of 35 points ($b$ filter measurements of Table 2) distributed on 12 + 3 nights. Those differential magnitudes have been analysed by Fourier techniques (Deeming 1975) up to a frequency of 10 day$^{-1}$. A peak clearly stands out at the frequency of $\nu_1 = 0.392$ day$^{-1}$ ($P = 2.551$ day, see Fig. 1). It is interesting to notice that its width is slightly larger than the natural width which must be $\Delta\nu = 1/T = 0.09$ day$^{-1}$ (where $T$ is the total length in time of the data string; the three isolated nights are too far from the other points to be of some practical influence on the spectral window). The use of the method of Scargle (1982) permits an estimation of the significance level (SL) associated with this peak to be obtained. We derive an SL of 0.0025 which indicates that a deeper analysis is justified.

**Table 5.** Observations corresponding to run No. 2.

| JD 2440000+ | $b-y$ | $y$ |
|---|---|---|
| 6099.7772 | −0.1784 | 0.8566 |
| 6099.8268 | −0.1806 | 0.8638 |
| 6100.7877 | −0.1983 | 0.8984 |
| 6101.7600 | −0.1624 | 0.8517 |
| 6102.8070 | −0.2064 | 0.9086 |
| 6103.8329 | −0.1748 | 0.8492 |
| 6104.7319 | (−0.1381) | (0.6813) |
| 6105.8564 | −0.1899 | 0.8728 |
| 6106.7411 | −0.1973 | 0.8888 |
| 6107.8330 | −0.1762 | 0.8673 |
| 6108.6222 | −0.1996 | 0.8845 |
| 6110.6151 | −0.1741 | 0.8874 |
| 6111.6272 | −0.1704 | 0.8477 |
| 6112.6807 | −0.1856 | 0.8594 |
| 6113.5765 | −0.2038 | 0.9108 |

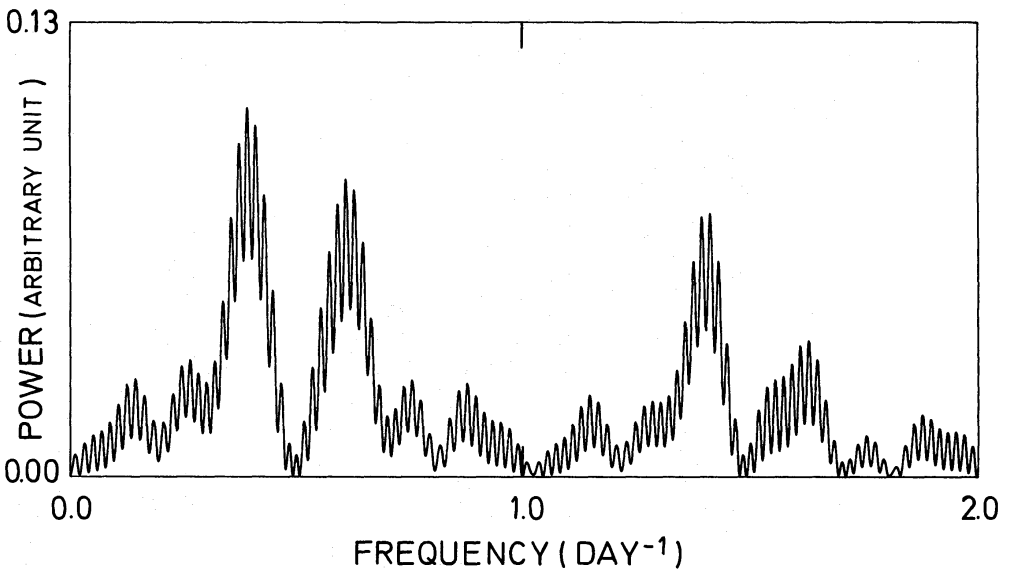


**Figure 1.** Power spectrum of the $b$ differential magnitudes contained in dataset I [Deeming's (1975) method]. A peak at $\nu = 0.392$ day$^{-1}$ and its aliases clearly dominate.

The data have been pre-whitened for this periodicity and re-analysed. The term of pre-whitening is defined by Blackman & Tukey (1958). However, in the present paper, we use it in a less restrictive way. We simply mean that we remove from the data a sine wave (of the relevant frequency) whose semi-amplitude (i.e. the coefficient of the sine) and phase have been determined through a least-squares fit performed in the phase diagram. The relevant power spectrum is then dominated by a peak at $\nu_2 = 0.320$ day$^{-1}$ ($P = 3.125$ day) and the SL is, in this case, of 0.0008 indicating again a marked feature. It thus appears that, in the original dataset, the two frequencies were present and blended; this explains the reported larger width for the peak corresponding to $\nu_1$. One should keep in mind that, due to the closeness of the two frequencies, the position of the two peaks in the power spectrum can be shifted due to mutual interactions and consequently may not correspond to the true frequencies (Loumos & Deeming 1978). A non-linear least-squares fit is necessary to derive more accurate frequencies. It may be worth pointing out that, at first sight, one would expect the SL associated with $\nu_1$ to be lower (i.e. better rejecting the white noise hypothesis) than the one associated with $\nu_2$ as the peak at

$\nu_1 = 0.392$ day$^{-1}$ ($P = 2.551$ day) is markedly higher than the one at $\nu_2 = 0.320$ day$^{-1}$ ($P = 3.125$ day). However, we obtained $SL_{\nu_1} = 0.0025$ against $SL_{\nu_2} = 0.0008$. The reason is that the value of 0.0025 is poorly estimated because, during this first step, the variance brought by $\nu_2$ is considered as noise. This situation is in fact a good hint that, at a significance level of 0.0008, there exist at least two frequencies in the data.

The pre-whitened data have been pre-whitened again, this time for $\nu_2$, and re-analysed. A third periodicity $\nu_3 = 0.143$ day$^{-1}$ ($P = 6.993$ day) is present at an SL of about 0.0150. This periodicity is not markedly smaller than the length of the run and extreme caution is necessary. Here also, the position of the peak in the power spectrum can be vitiated. The data have been pre-whitened for the third frequency and then no new periodicity could be detected. In summary, the dataset I suggests the simultaneous presence of three frequencies in the variability of WR40. Therefore, we performed a three sine non-linear (semi-amplitudes, phases and frequencies as free parameters) least-squares fit to the data and we obtained the following frequencies and semi-amplitudes

$\nu_1 = 0.388$ day$^{-1}$ ($P = 2.577$ day) $\quad a_1 = 0.022$ mag

$\nu_2 = 0.319$ day$^{-1}$ ($P = 3.135$ day) $\quad a_2 = 0.015$ mag

$\nu_3 = 0.165$ day$^{-1}$ ($P = 6.061$ day) $\quad a_3 = 0.012$ mag.

As already mentioned, the latter values should be more reliable. Only the third frequency appeared to be strongly shifted from the value derived on the basis of the power spectrum. The above fit is illustrated in Fig. 2; its quality is a good argument in favour of the real existence of the three periodicities. In addition, the combination of the three semi-amplitudes can explain the reported 0.1 mag peak-to-peak variability for this star. However, 12 + 3 nights are not enough to test the consistency of the three frequencies. In other words, we could be dealing with a particular realization of a random process; data in limited number are, of course, always expandable in such Fourier series. In order to get more information on that star we have analysed other datasets.

Before discussing them, it may be worth pointing out that the present data (dataset I) were

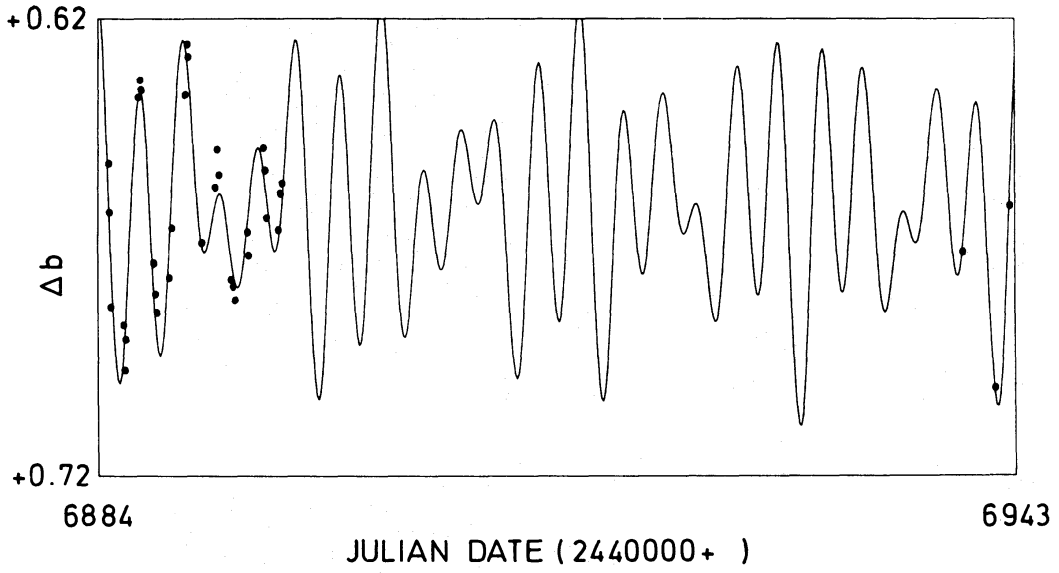


**Figure 2.** Variation of the Strömgren *b* filter differential magnitude of WR40 as a function of time. Dots represent the observations from dataset I and the continuous line is the fitted curve discussed in Section 3.1.1.

collected in such a way as to allow the search for higher frequencies. However, no outstanding peak occurs in the range 1.5–10 day$^{-1}$. All the peaks below 1.5 day$^{-1}$ are either the above quoted frequencies $\nu_i$ or their one-day aliases $1-\nu_i$ or $1+\nu_i$. There remain some uncertainties in the choice of the actual progenitor: we have always adopted the higher, i.e. the most likely, one. In the particular case of dataset I, it is always situated between 0.0 and 0.5 day$^{-1}$. Therefore, there is no evidence for short time-scale periodicity (2–16 hr). Clearly, nothing can be said about a more distant aliasing.

### *3.1.2 Dataset II*

Dataset II covers a longer time span than dataset I does: this corresponds to a natural width of $\Delta\nu = 0.012$ day$^{-1}$. The *b* differential magnitudes have been analysed also by Fourier techniques. A peak is clearly standing out at the frequency $\nu_1 = 0.157$ day$^{-1}$ ($P = 6.369$ day, see Fig. 3). The relevant SL as estimated by the method of Scargle (1982) is 0.15, which is not conclusive by itself. However, it is interesting to point out the compatibility of this frequency with the one labelled $\nu_3$ in dataset I (see Section 3.1.1). We have also analysed the data by using the trial period string length (TPSL) methods of Lafler & Kinman (1965) and of Renson (1978). The deepest dip in the periodograms is situated at $\nu_1 = 0.157$ day$^{-1}$ (see Fig. 4). The associated SL can be computed by the method of randomization proposed by Nemec & Nemec (1985); we obtain 0.19. All these results are in good agreement with the Fourier results. The semi-amplitude of the variation is about 0.011 mag which is close to the value obtained in dataset I.

A second frequency can be suspected at $\nu_2 = 0.474$ day$^{-1}$ ($P = 2.111$ day). In fact, this frequency dominates the power spectrum of the data after they have been pre-whitened for $\nu_1 = 0.157$ day$^{-1}$. Anyhow, the deviation from the null-hypothesis of white noise is still less significant for $\nu_2$ than for $\nu_1$. A fitted sine curve leads to a semi-amplitude smaller than 1 per cent.

The magnitudes corresponding to the *y* filter have equally been submitted to a detailed analysis. It appears that the outcoming frequency is again $\nu_1 = 0.157$ day$^{-1}$ ($P = 6.369$ day) with a semi-amplitude of about 0.017 mag and an SL of 0.049. The latter seems to indicate a

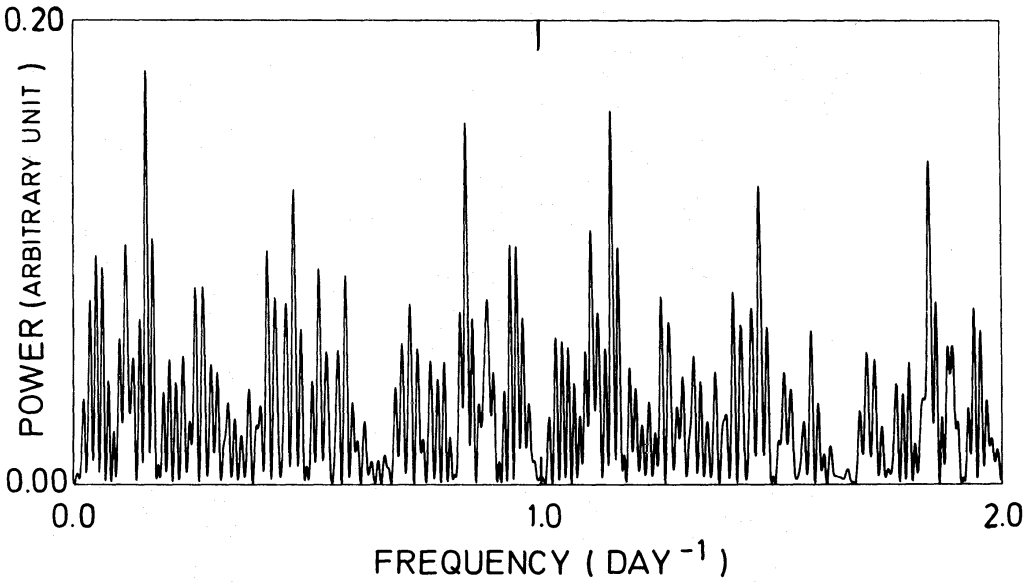


**Figure 3.** Power spectrum of the *b* differential magnitudes contained in dataset II (Deeming's (1975) method). A peak at $\nu = 0.157$ day$^{-1}$ and its aliases are clearly dominating.

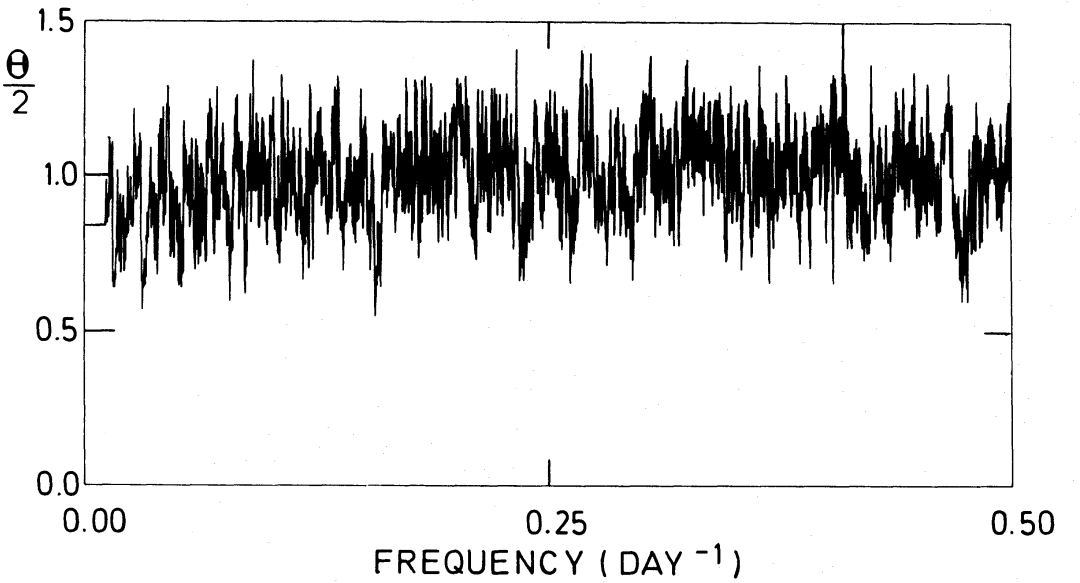


**Figure 4.** Periodogram of the *b* differential magnitudes contained in dataset II. Run of half the Θ statistic of Lafler & Kinman (1965) as a function of the frequency. The deepest dip is located at $\nu = 0.157$ day$^{-1}$ confirming the results from Fig. 3.

better marked deviation from randomness and a tendency for the star to exhibit the same kind of variation in both colours. The semi-amplitude seems to be slightly greater in the *y* which agrees with the conclusions of van Genderen *et al.* (1987). The possible presence of $\nu_1$ is confirmed by the TPSL methods.

The *y* magnitudes pre-whitened for $\nu_1$ have been re-analysed. The Fourier techniques put forward a second frequency at $\nu_2 = 0.475$ day$^{-1}$ ($P = 2.105$ day) in good agreement with our results on the *b* filter, whereas TPSL methods show a marked preference for another frequency, namely 0.237 day$^{-1}$ ($P = 4.219$ day). Nevertheless, none is statistically significant and, at this level, one may not be surprised to get diverging conclusions from the application of the two kinds of methods.

### *3.1.3 Dataset III*

The interpretation of the power spectrum relevant to dataset III is less straightforward than for the previous cases. Nevertheless, one can tentatively set up a list of three families of aliases. The most noticeable one consists in peaks located at $\nu = 0.027$ day$^{-1}$, $\nu = 0.974$ day$^{-1}$ and $\nu = 1.975$ day$^{-1}$, the second peak being the highest one. If one neglects the fact that we are beyond 0.5 day$^{-1}$, the relevant SL would be 0.028. This family is also detected by TPSL methods, for which the approach of Nemec & Nemec (1985) leads to an SL associated to $\nu = 0.027$ day$^{-1}$ of 0.07. The second family gathers $\nu = 1.053$ day$^{-1}$ and $\nu = 1.064$ day$^{-1}$, which are clearly related, and their respective aliases. The powers of those peaks are slightly less than those of the first family but are highly dependent on whether or not the first trend has been removed from the data. Moreover, the present family also dominates the power spectrum of the differential magnitudes between the comparison stars. This could indicate an observing and/or instrumental artefact. Nevertheless, one should stress that the above-mentioned families cannot be properly studied on the basis of dataset III alone because their low frequency member corresponds to a period of the order of, or greater than, the longest uninterrupted run of observations. As one has to deal with low amplitudes of variation, one has to be cautious. The third family, less well marked, consists of $\nu = 0.190$ day$^{-1}$ and its aliases.

Owing to the above-mentioned discussion, we decided to retain, as a first frequency for dataset III, $\nu_1 = 0.974$ day$^{-1}$ ($P = 1.027$ day). The choice of the alias is somewhat arbitrary but taking the highest peak permits a better pre-whitening process when utilizing a simple sine curve to model the variation.

The data have been pre-whitened for $\nu_1$, and re-analysed. In the resulting dataset, the power of the peaks belonging to the second family is markedly decreased, which could indicate some interaction between the latter and the first family. The effect is such that the third family is now as powerful as the second one. Owing to our above-mentioned remarks on the possible origin of the latter, we retain $\nu_2 = 0.190$ day$^{-1}$ ($P = 5.263$ day). It should be mentioned that its alias $1 - \nu_2 = 0.811$ day$^{-1}$ is as powerful as the arbitrarily selected progenitor. The related SL is around 0.12 following Scargle's (1982) method. The $\nu_2$ frequency corresponds also to the deepest dip in the Lafler & Kinman (1965) and Renson (1978) periodograms but the deviation is totally insignificant.

Finally, we have analysed the *y* filter data. The first frequency retained is $\nu_1 = 2.065$ day$^{-1}$ ($P = 0.484$ day); the choice of the alias is arbitrary and based on the height of the peak in the power spectrum. Let us note that this family of aliases was also visible in the *b* filter data. The second frequency is $\nu_2 = 0.205$ day$^{-1}$ ($P = 4.878$ day) whose alias $1 + \nu_2 = 1.205$ day$^{-1}$ is rather high. The second frequency is clearly related although slightly different from the $\nu_2 = 0.190$ day$^{-1}$ noticed in the *b* filter data.

### 3.2 ANALYSIS OF PREVIOUSLY PUBLISHED DATA

As the analysis of the same data by different groups (MI or Smith *et al.* 1985) led to incompatible results, we decided to re-analyse some of the previously published data. This also allows a more homogeneous study of observations spread on a very long time basis, namely 1975 to 1987.

#### *3.2.1 Dataset IV (MI)*

The dataset IV consists of the narrow-band photometry published by MI and re-analysed by Smith *et al.* (1985) (precisely, runs of 1975 and 1976, i.e. tables 2 and 3 of MI). The natural width is $\Delta\nu = 0.0022$ day$^{-1}$ although each run independently has a natural width of about $\Delta\nu = 0.028$ day$^{-1}$. The power spectrum computed by the discrete Fourier transform method of Deeming (1975) is dominated by a peak at $\nu = 0.167$ day$^{-1}$. A non-linear (semi-amplitude, phase and frequency as free parameters) least-squares fit as well as the method of Scargle (1982) favour a value of $\nu_1 = 0.170$ day$^{-1}$ ($P = 5.882$ day), which we adopt. The associated SL is 0.018 and the semi-amplitude is 0.019 mag for the filter centred at 5640 Å. This is interesting and agrees well with the analysis performed on the same dataset by Smith *et al.* (1985) and also by van Genderen *et al.* (1987). The latter, in particular, find the largest correlation coefficient for $P = 6.05$ day, a value of the period not significantly different from the one reported here. This frequency $\nu_1$ is also visible as the deepest dip in the periodograms corresponding to the TPSL methods of Lafler & Kinman (1965) and of Renson (1978) but the method of Nemec & Nemec (1985) teaches us that the relevant deviation is insignificant.

The data pre-whitened for $\nu_1 = 0.170$ day$^{-1}$ have been re-analysed. The power spectrum and the periodograms of the pre-whitened data are quite noisy and nothing statistically significant can be derived. The highest peak in the power spectrum is situated at $\nu_2 = 0.423$ day$^{-1}$ ($P = 2.364$ day) although no clear dip is present in the periodograms at this location. This frequency is also detected by van Genderen *et al.* (1987) and is also the main original frequency resulting from the analysis of MI. It has been discarded by Smith *et al.* (1985) on the

basis that the associated features were weak and variable. The absence of any corresponding features in our periodograms seems to give some support to their assertion. Besides this, our periodograms exhibit two small dips around $\nu = 0.29$ day$^{-1}$ and around $\nu = 0.36$ day$^{-1}$, whereas a peak is visible in the power spectrum at $\nu = 0.32$ day$^{-1}$. The latter is also present in the power spectrum of the data pre-whitened for $\nu_2$ and could indicate the presence of a third frequency $\nu_3 \sim 0.32$ day$^{-1}$ ($P \sim 3.1$ day). The associated deviation is of course insignificant, but the position in frequency is in rather good agreement with the conclusions of Smith *et al.* (1985) about the presence of a second periodicity at $P = 2.8396$ day. However, our analysis does not permit a precise frequency derivation and seems to indicate that the effect is somewhat fuzzy. Particularly, we would not be as categorical as Smith *et al.* (1985) in discarding the possibility that $\nu_3$, if existing, is the harmonic of $\nu_1$.

### *3.2.2 Dataset V (LM)*

Dataset V consists of the $V$ magnitudes published by LM. The mere inspection of their fig. 3(b) shows that data from some nights, such as JD 2446164 and JD 2446165, depart from the local mean. The Fourier methods are sensitive to those particular features and a strong peak appears at $\nu = 0.5$ day$^{-1}$. As it concerns a small number of points with high amplitudes, this effect has almost no influence on the periodograms. We decided to remove the effect even if its origin is not clear. As a consequence, both the power spectrum and the periodograms agree to exhibit the same two frequencies. The first one is situated at $\nu_1 = 0.111$ day$^{-1}$ ($P = 9.009$ day) and corresponds to a significance level of 0.042 following Scargle's (1982) method and of 0.04 following Nemec & Nemec's (1985) one. The relevant variation is easily visible in fig. 3(b) of LM and corresponds to an asymmetry between the two sides of the observational gap situated around JD 2446155–2446156. The dip at $\nu_1$ in the periodograms is by far narrower than the natural width of $\Delta\nu = 0.058$ day$^{-1}$, which could indicate some problems.

The second frequency present is situated at $\nu_2 = 0.211$ day$^{-1}$ ($P = 4.739$ day) and exhibits the natural width. It is the frequency reported by LM.

## 3.3 GLOBAL RESULTS

None of the analysed datasets indicates the existence of a true periodicity which is significant by itself. As the situation could be confused, we have gathered in Fig. 5 the results of our analyses. The positions of the different noticed frequencies are given for each analysed dataset. The frequencies corresponding to a detection with an SL lower than 0.05 are outlined. At the extreme right part, we have summarized the suggestions and results of already published period analyses. It is clear that, for dataset V and perhaps III, we find only marginal evidence of the periods proposed by Moffat (1983) and LM. No evidence is found in other datasets. However, as long as the main frequency is concerned, we agree with the conclusions of Smith *et al.* (1985) when we analyse the same dataset (IV) and we bring further evidence for the possible existence of a periodicity around 6 day on the basis of two new datasets, namely I and II. The mere suggestion of the existence of the same period in three datasets corresponding to three separate epochs is most interesting, since it could indicate the presence of a unique, more or less stable, consistent phenomenon, the signature of which is mixed and sometimes completely overwhelmed by other types of variations. It is necessary to check for the coherence of this signature; this means that we have to verify whether or not the reported variability has some property of phase coherence as a strictly periodic phenomenon would have. Recurrent pseudoperiodic phenomena can induce the same apparent period in different datasets. It is unlikely that they keep a phase coherence. A rigorous test of the coherence seems to be

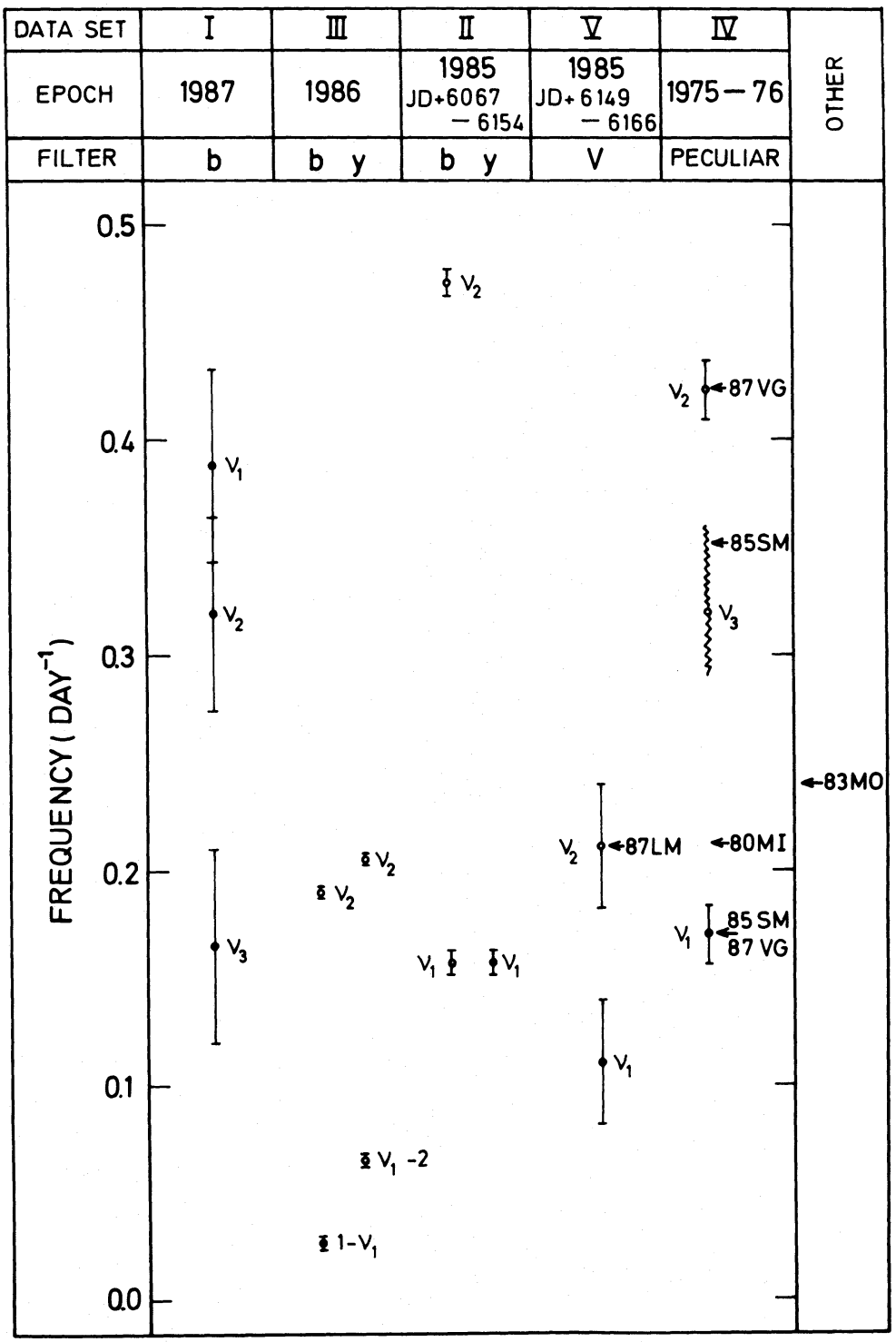


**Figure 5.** Synopsis of the results of our study. The positions of the different noticed frequencies are given for each analysed dataset. Black dots indicate that the relevant significance level was lower than 0.05. White dots correspond to less significant frequencies. The full error bars correspond to the natural widths of the peaks (see text). A special symbol (wave) is used for $\nu_3$ in dataset IV, as this frequency is ill-defined (see Section 3.2.1). The horizontal arrows indicate the position of the previously suggested frequencies for the dataset under consideration. The meaning of the symbols is the following: 87LM = Lamontagne & Moffat (1987); 80MI = Moffat & Isserstedt (1980); 85SM = Smith *et al.* (1985); 87VG = van Genderen *et al.* (1987). The last column (83MO = Moffat 1983) corresponds to a radial velocity analysis, not to a photometric analysis.

beyond our possibilities. The best thing to do then is to put all the datasets together and to verify whether or not the individual periodicities around 6 day combine themselves in a constructive way. Consequently, we removed the mean and first trend of each dataset and put them together. Then a Fourier analysis of dataset I + II + III + IV + V as a whole was performed and the relevant power spectra are given in Figs 6 and 7. Fig. 6 corresponds to the utilization, in datasets II and III, of the *b* filter data, whereas Fig. 7 deals with the utilization of the *y* filter data. In both figures, the power spectrum is dominated by one family of aliases which is near the expected position. A periodicity is clearly detected: we derive a value of $\nu_A = 0.160 \pm 0.002 (1\sigma)$ day$^{-1}$ ($P = 6.250 \pm 0.078$ day) where the standard deviation has been computed using Kovacs's method (Horne & Baliunas 1986). The 10-yr aliasing is too tight to permit the removal of the ambiguity and has therefore been neglected. A 1-yr aliasing is

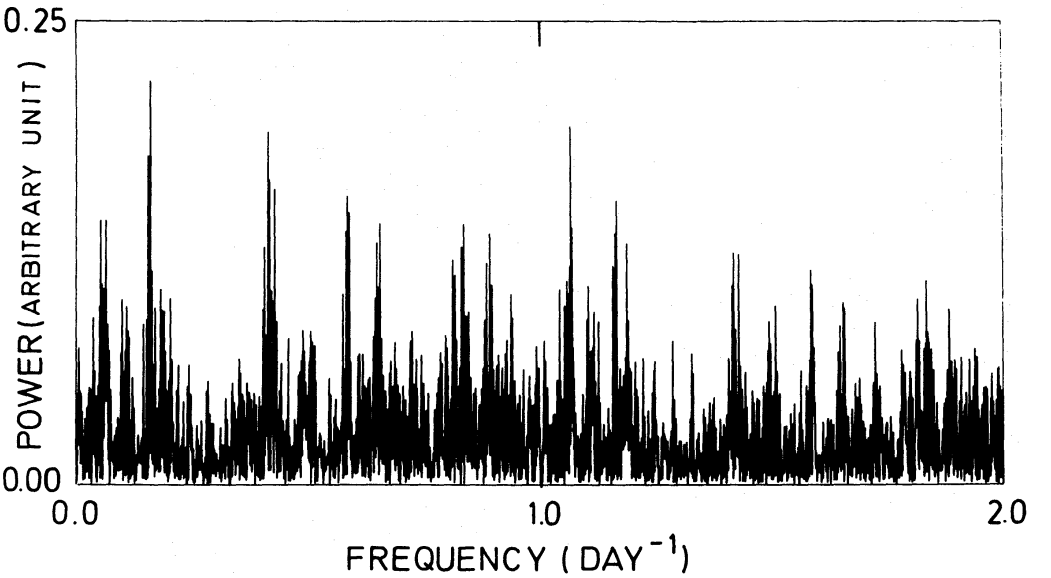


**Figure 6.** Power spectrum for WR40 (Deeming's (1975) method). The filter used for datasets II and III is Strömgren's *b* filter.

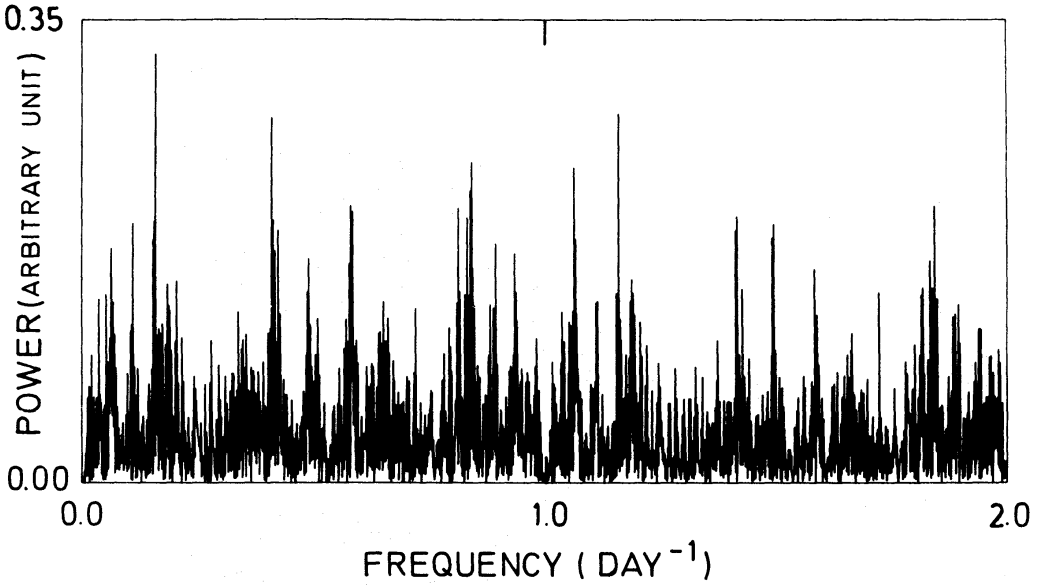


**Figure 7.** Power spectrum for WR40 [Deeming's (1975) method]. The filter used for datasets II and III is Strömgren's *y* filter.

also present and we cannot reject an alias situated at $\nu = 0.158$ day$^{-1}$. However, it is worth mentioning that this alias is within one standard deviation of the selected peak. The significance level associated with $\nu_A$ and computed following Scargle's (1982) method is always between 0.005 and 0.0003, depending on the selected 10-yr alias and on the particular choice of the different filters for each dataset. Such small probabilities indicate that some kind of coherence plays a role: the peaks relevant to each dataset combine themselves in a constructive way. Nevertheless, the great unevenness of the sampling allows to cast some doubt on the adopted number of degrees of freedom involved in the computation of the significance level (Horne & Baliunas 1986). Therefore, we have performed simulations of a great number of complete datasets of white noise 'observations' mimicking the magnitude distribution of the data. For each simulated dataset, we have searched for the highest peak in the power spectrum. From the distribution of the heights of those peaks, we deduce a strong upper limit of 0.010 for the significance level. Therefore, we believe that the actual presence of a deterministic, dominantly periodic process is beyond any doubt. A fitted sine curve to the data leads to a semi-amplitude (essentially in $b$) of about 0.010 mag, a value in good agreement with the power in the peak visible in Fig. 6 and with what is found for individual datasets.

As the observed peak-to-peak variability of WR40 is 0.1 mag, it is evident that the deterministic, dominantly periodic, process reported here is responsible for a small part of the total variations and that it is in fact hidden in (one) other process(es), at least partially stochastic. In fact, Fig. 5 shows that $\nu_A$ dominates in two datasets (II and IV), appears in another one (I) and seems to be missing in the two others (III and V). This clearly indicates that the signature of the phenomenon which is responsible for the long-term stability of a 6-day periodicity is, at some epochs, completely overwhelmed by ephemeral pseudoperiodic variations or dominated by apparently pure noise.

We have also analysed the data with the TPSL methods of Lafler & Kinman (1965) and of Renson (1978). No frequency can be outlined. However, the failure of obtaining any result via

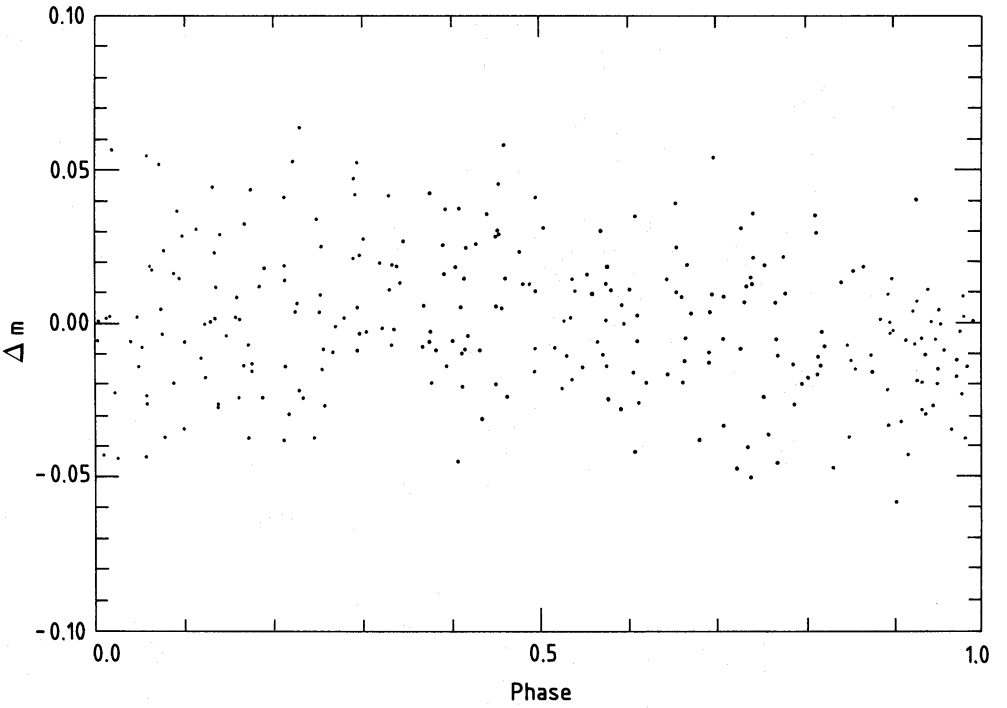


**Figure 8.** The modified (see Section 3.3) magnitudes of dataset I + II + III + IV + V folded in a phase diagram with $P = 6.250$ day.

those methods is understandable because the periodic process is deeply imbedded in (an)other process(es) of variation. This implies that the phase diagram of any dataset (even one in which the period is easily found) appears extremely noisy. As an example, Fig. 8 shows all the data folded with $P=6.250$ day.

The data as a whole (I + II + III + IV + V) have been pre-whitened for $\nu_A$ and re-analysed. A second family of aliases dominates the power spectrum. In fact, this family is already visible in the original data (see particularly Fig. 6). The associated frequency is $\nu_B=0.413$ day$^{-1}$ ($P=2.421$ day) for the data of Fig. 6 and $\nu_B=0.420$ day$^{-1}$ ($P=2.381$ day) for the ones of Fig. 7. The shift between the two frequencies is not real and is easily explained in terms of noise effects on the height of 1-yr aliases of the same frequency. The significance level associated with $\nu_B$ and corrected for the particular sampling of the data is always comprised between 0.08 and 0.01. The result is interesting but inconclusive: it is not possible to decide here whether or not we have to deal with a second stable periodic variation.

Clearly, the main contribution to $\nu_B$ comes from the second frequency (not significant by itself) visible in dataset IV with probably some influence of the dominating frequency in dataset I; the three other datasets (II, III and V) give no support to $\nu_B$.

One striking fact in Fig. 5 is the great similarity between the frequency patterns shown by datasets I and IV. We have also analysed the data of Table 5 (run No. 2) and, although to a smaller extent, they show some tendency to exhibit the same behaviour. Unfortunately, nothing more could be deduced from these data. The observed frequency pattern could be due to the deep nature of the variability but the amount of data available is not large enough to permit firm conclusions beyond the existence of $\nu_A$. The data have been pre-whitened for $\nu_B$ and re-analysed. No new frequency can be detected but several peaks appear for some frequencies that have been mentioned in the case of individual datasets.

## 4 Discussion and conclusion

Recent studies (van Genderen *et al.* 1987; Lamontagne & Moffat 1987) have shown that most of the WR, mainly the late WN, stars are photometrically variable. It is also well known that in most of the WR stars, the surface is hidden by the dense wind flowing from these objects, a wind which in some cases can also completely hide a close binary system. There is no reason to believe that, even for a single object, this flow of matter is time independent and, at a given moment, spherically symmetric. We are thus facing an interesting challenge: unravel some physical characteristics of an object which is mostly hidden by a time-dependent phenomenon. The variability of the wind can provide some insight if it is controlled by a deeply rooted mechanism like the rotation of a stable surface inhomogeneity, the distortion by the presence of a close companion or some kind of stable pulsations. Unfortunately, other sources of variability are probably present, such as dynamical instabilities of the flow or ephemeral activity at the surface of the star. Although most of the wind perturbations generated by this second variety of phenomena must be completely erratic and consequently only increase the 'noise' level, we cannot *a priori* exclude that some of them exhibit a pseudoperiodic character on a time-scale of a few pseudoperiod lengths, i.e. on the time-scale of a typical observing run if the pseudoperiod is of the order of a few days. What then could be the signature of a variability linked to a deeply rooted characteristic of the hidden object? First, the recurrence of the same period(s). Secondly, more stringent, is the stability of the phase. A deeply rooted and stable mechanism may be completely hidden during some observing runs. Nevertheless, every time its signature shows up, its phase must be kept if we are dealing with a binary, or with a rotation (e.g. through relatively stable inhomogeneities at the surface) or with fairly stable pulsation phenomena.

How does this apply to WR40? First of all, the recurrence of the same period. One period of the order of 6.25 day (see the error bars on Fig. 5) shows up in three different datasets (namely I, II and IV) widely separated in time as they correspond respectively to 1987, 1985 and 1975–76. Consequently, this period is a good candidate for a test with the second criterion, i.e. phase coherence. As the phenomenon is deeply imbedded in other less deterministic variations, such a test is difficult to perform in a rigorous way. However, the results of our analysis show that such a coherence seems to be kept on a large time-scale. Effectively, the different datasets combine in a constructive way and the periodicity shows up more significantly in the whole dataset, leading to a probability less than 1 per cent to get such a result by mere chance. As a consequence, it seems reasonable to consider that the phenomenon exhibiting a periodicity of the order of 6.25 day ($\nu_A = 0.160$ day$^{-1}$) at three different epochs is not a pseudoperiodic instability taking place from time to time in the wind but, on the contrary, is linked to a variability taking place in the very core of WR40. The true nature of that phenomenon is difficult to ascertain. We have to keep in mind that its signature has a semi-amplitude of about 10 per cent of the total peak-to-peak variation. Nevertheless, the fact that the periodicity is detected in different filters and that the phase coherence seems to be kept independently of the filter taken into account is worth pointing out. It seems to indicate that the photometric variations observed in a given filter are not induced by the intensity variations of some peculiar emission line but are most probably due to continuum variations as suggested by van Genderen *et al.* (1987) in their analysis of multicolour photometry. Taking into account the length of the period, the easiest explanation presently is rotation either of a binary system or of a single object with a relatively stable inhomogeneous surface. A phenomenon linked to pulsations is presently less likely, if we refer to the theoretical modelling of the WR stars, as all the predicted periods are markedly much shorter (Maeder 1985; Scuflaire & Noels 1986). The only possibility would be a beat period exhibiting a remarkable stability. Insight into this intricate problem will require still more perseverance, particularly to definitively confirm or reject the existence of the second frequency, $\nu_B = 0.413$ day$^{-1}$. In this context, it is interesting to notice that, if $\nu_A$ is considered as the beat frequency and $\nu_B$ as one of the fundamental ones, the other fundamental frequency could be $\nu_C = \nu_A + \nu_B \sim 0.57$ day$^{-1}$ which would be blended with the 1-day alias $1 - \nu_B$ of $\nu_B$.

## Acknowledgments

Part of the data were obtained, in the framework of the 'Long-term Photometry of Variables' programme at ESO, by H. Duerbeck, O. Stahl, F. Dekker, F.-J. Zickgraf, M. Burger, A. Jorissen, D. Steenman and R. Madejski. We are greatly indebted to all of them for their observational contribution. This work has been partly supported by the Belgian Fund for Scientific Research (FNRS/NFWO) through research grants to JM, CS and JMV. Allocation of computer time by the Computing Centre (SEGI) of the University of Liège is also gratefully acknowledged. Last but not least, our thanks go to J.-P. Swings who has read and significantly improved the manuscript.

## References

Blackman, R. B. & Tukey, J. W., 1958. *The Measurement of Power Spectra,* Dover, New York.
Chu, Y.-H., Treffers, R. R. & Kwitter, K. B., 1983. *Astrophys. J. Suppl.,* **53,** 937.
de Loore, C. & de Grève, J.-P., 1975. *Astrophys. Space Sci.,* **35,** 241.
Deeming, T. J., 1975. *Astrophys. Space Sci.,* **36,** 137.
Drissen, L., St-Louis, N., Moffat, A. F. J. & Bastien, P., 1987. *Astrophys. J.,* **322,** 888.

Horne, J. H. & Baliunas, S. L., 1986. *Astrophys. J.,* **302,** 757.
Lafler, J. & Kinman, T. D., 1965. *Astrophys. J. Suppl.,* **11,** 216.
Lamontagne, R. & Moffat, A. F. J., 1987. *Astr. J.,* **94,** 1008.
Loumos, G. L. & Deeming, T. J., 1978. *Astrophys. Space Sci.,* **56,** 285.
Maeder, A., 1985. *Astr. Astrophys.,* **147,** 300.
Manfroid, J., 1985. Traitement numérique des données photométriques, *thèse de doctorat spécial,* Université de Liège.
Manfroid, J., Gosset, E. & Vreux, J.-M., 1987. *Astr. Astrophys.,* **185,** L7.
Moffat, A. F. J., 1983. In: *Wolf–Rayet Stars: Progenitors of Supernovae?, Proc. Meudon Workshop,* p. III.13, eds Lortet, M.-C. & Pitault, A.
Moffat, A. F. J. & Isserstedt, J., 1980. *Astr. Astrophys.,* **91,** 147.
Nemec, A. F. L. & Nemec, J. M., 1985. *Astr. J.,* **90,** 2317.
Renson, P., 1978. *Astr. Astrophys.,* **63,** 125.
Scargle, J. D., 1982. *Astrophys. J.,* **263,** 835.
Scuflaire, R. & Noels, A., 1986. *Astr. Astrophys.,* **169,** 185.
Smith, L. J., Lloyd, C. & Walker, E. N., 1985. *Astr. Astrophys.,* **146,** 307.
Sterken, C., 1983. *The Messenger,* **33,** 10.
Tutukov, A. & Yungelson, L., 1973. *Nauchn. Inform.,* **27,** 3, 58, 70, 86.
van den Heuvel, E. P. J. & Heise, J., 1972. *Nature Phys. Sci.,* **239,** 67.
van der Hucht, K. A., Jurriens, T. A., Olnon, F. M., Thé, P. S., Wesselius, P. R. & Williams, P. M., 1985. *Astr. Astrophys.,* **145,** L13.
van der Hucht, K. A., Hidayat, B., Admiranto, A. G., Supelli, K. R. & Doom, C., 1988. *Astr. Astrophys.,* **199,** 217.
van Genderen, A. M., van der Hucht, K. A. & Steemers, W. J. G., 1987. *Astr. Astrophys.,* **185,** 131.
Vreux, J.-M., 1987. In: *Instabilities in Luminous Early Type Stars,* p. 81, eds Lamers, H. J. G. L. M. & de Loore, C., Reidel, Dordrecht.